Effect of Asperity Height on Wear Behavior by Finite Element Method

Ahmed Hadi Abood
Pumps Eng. Dept. , Technical College - AlMusaib

Abstract

This paper presents an investigation of contact surface interface, which is of strong interest for wear applications. The prediction of the wear depth in contact surfaces is thus a challenging task. The effect of the asperities height (0.045, 0.055, 0.065, and 0.07)mm, the applied forces and the shape of the contact surfaces on the wear depth and contact pressure are investigated by finite element method via ANSYS software. Wear simulation approach based on Archard's model was proposed, in which ANSYS was used to simulate the progressive accumulation of wear between contact surfaces. Results showed that the wear behavior can be simulated with the series of discrete models and the method proposed can be widely used to predict wear problems for engineering. Two cases are studied, the first one is for rectangular contact surfaces and the other for circle- rectangle contact surfaces with different height of asperities. It was also concluded that the increased of contact's time caused the wear depth for different asperities increased and vice versa for contact pressure.

Keywords: wear simulation , Archard model, finite element model, ANSYS software, contact pressure

الخلاصة

تمت الدراسة باستخدام طريقة العناصر المحددة. فقد تم التنبؤ بعمق البلى في الأسطح المتلامسة. حيث انه تم دراسة تأثير ارتفاع asperities (0.045 ، 0.055 ، 0.065 ، 0.07) ملم والقوى المسلطة على عمق البلى وشكل اسطح التلامس بواسطة طريقة العناصر المحددة من خلال برنامج ANSYS. حيث انه تم محاكاة العملية باستخدام نموذج المحاكاة على أساس نموذج Archard. وقد بينت النتائج أن سلوك البلى يمكن أن تكون محاكاة لسلسلة من النماذج المتميزة، وأن الطريقة المقترحة هي الافضل على نطاق واسع للتنبؤ بمشاكل البلى الهندسية . فقد تم دراسة حالتين، الأولى هي للأسطح المتلامسة ذات شكل مستطيل والآخر للأسطح المتلامسة ذات شكل دائرة – مستطيل. ولقد بينت الدراسة انه عند زيادة وقت التلامس فان عمق البلى سوف يزداد ويقل ضغط التلامس.

Symbols

V….. wear volume
x ….. sliding distance
w ….. normal load
H ….. hardness of the surface
K ….. dimensionless wear rate
p ….. contact pressure
$W_{int.}$ ….. internal work (strain energy)
$W_{ext.}$ …. external work (work done by the applied force)
$\{\varepsilon\}$ ….. elements of virtual strain vector
$\{\sigma\}$ ….. elements of real stress vector
dV ……. infinitesimal volume of the element
$[D]$ ……. constitutive matrix
$[N]$ ……. shape function matrix
$\{a\}$ …… unknown nodal displacements vector (local displacements)
$\{U\}$ …… body displacements vector (global displacements).
$[B]$ ……. strain-nodal displacement relation matrix, based on the element shape functions
$\{F\}$ …….. nodal forces applied to the element
T_n ………. tolerance (taken equal to 0.1%)

{R} …….. residual load vector

Introduction

The simplest definition of the wear is the collapse of the friction's surfaces as a result of mechanical action (Rabinowicz, 1965),or is a loss of material from one of the contact surfaces or both together when they are under the influence of relative movement (هولنك، 1985). In general, the wear occurs naturally between any two contact surfaces where the relative movement between them is existed and can not prevent wear once and for all because it usually appears whenever load with the movement, thus wear is the progressive loss of substance from the operating surfaces of a body occasionally as a results of relative motion at the surfaces.

Kim el al., (2005) describes the estimation method of die service life based on wear and the plastic deformation of dies in hot forging processes. Nam Ho Kim et al., (2005) proposed a numerical approach that simulates the progressive accumulation of wear in oscillating metal on metal contacts , the approach uses a reciprocating pin- on – disk Tribometer to measure a wear rate for the material pair of interest. Biglari and Zamani , (2008) examined the wear profile on the die surface during the hot forging operation for axisymmetric cross- section experimentally and using finite element method. Xuejin SHEN et al., (2010) presented the numerical simulation of sliding wear based on Archard Model. Wang and Masood (2011), investigated the effects of draw die geometry on the sheet metal tool wear distribution over the draw die radius using numerical and experimental methods, a numerical tool wear model is introduced and applied using ABAQUS package. In this paper, a procedure is proposed whereby the effects of the asperities height at wear process may be calculated for different contact surfaces shapes. The Archard equation is used as the basis for calculating wear depth by ANSYS software.

Archard Wear Model

The asperities are assumed to have a conical form as in Fig.(1), assumed that a hard surface sliding over a softer materials. Consider a single asperity of conical form is:

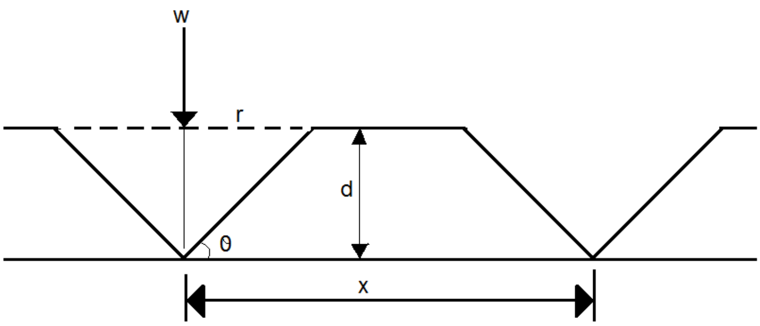

Fig.(1) The asperities according to Archard Wear Model(Johnson)

The vertical projected area of the conical asperity is a circle of radius (r) :-

Let the slop of the side of an asperity = θ , and the radius of circle of penetration in the face surface is = r , and let the depth of penetration = d .

$$\therefore \quad \tan\theta = \frac{d}{r} \qquad \text{……………………………. (1)}$$

The cross- sectional area of the triangular wear groove $= \frac{r}{2} \cdot d \cdot 2 = r \cdot d$ … (2)

But $d = r\ tan\theta$

$\therefore\ \ the\ area = r^2\ tan\theta$ .... (3)

Let the mean flow stress resisting the deformation equal $P_m \approx H$

where H is the hardness (for most materials $P_m \approx H$)

the force resisting sliding for a single asperity = $P_m\ r^2\ tan\theta \approx H\ r^2\ tan\theta$ .. (4)

the total friction force (F) = $\sum H\ r^2\ tan\theta$ .... (5)

$= H.tan\theta \sum r^2$ .... (6)

$$\therefore\quad F = \frac{H\ tan\theta}{\pi}\sum \pi r^2 \quad ....\ (7)$$

$$\text{Or}\quad F = \frac{H\ tan\theta}{\pi}(A) \quad ....\ (8)$$

Where A is the sum of the individual circles of penetration into the surface, or the real constant area.

Since, the normal load on a single asperity (w) is supported by the front – half only of the conical indentation .

$$w = P_m\frac{\pi r^2}{2} \quad ....\ (9)$$

The total load is :-

$$w = \sum w = \sum P_m\left(\frac{\pi r^2}{2}\right) = \sum H\left(\frac{\pi r^2}{2}\right) \quad ....\ (10)$$

$$w = \frac{H}{2}\sum \pi r^2 \quad ....\ (11)$$

$$w = \frac{H}{2(A)} \quad ....\ (12)$$

The coefficient of friction $\mu = \frac{F}{w} = \frac{H.tan\theta.(A)}{\pi.\frac{H}{2}.(A)} = \frac{2}{\pi}\ tan\theta$

Now, the volume of material removed is :-

$\delta V = r.d.x \rightarrow r^2 tan\theta.x$

Where x is a sliding distance

$$V = \sum r^2.tan\theta.x \quad ....\ (13)$$

$$V = \frac{x.tan\theta}{\pi}\sum r^2.\pi \quad ....\ (14)$$

$$V = \frac{x.tan\theta}{\pi(A)} \quad ....\ (15)$$

But from Eq.(12) , $A = \frac{2w}{H}$ .... (16)

$$\therefore\quad V = \frac{2\ tan\theta}{\pi}\left(\frac{w.x}{H}\right) \quad ....\ (17)$$

Or $V = K\left(\frac{w.x}{3H}\right)$ .... (18)

Where $K = \frac{6\tan\theta}{\pi}$ .... (19)

i.e. K is a function of surface topography.

Eq.(18) can be rewritten as

$$\frac{V}{x} = K\frac{w}{H} \qquad \text{.. (20)}$$

For simulation the evaluation of contact surface, it is essential to calculate the wear depth, this can be get from Eq.(20). The incremental of sliding distance is (Archard, 1953) :

$$\frac{dV}{dx} = K\frac{w}{H} \qquad \text{...................................... (21)}$$

Dividing Eq.(21) by ΔA , it can be get :

$$\frac{dV}{dx.\Delta A} = K\frac{w}{H.\Delta A} \qquad \text{...................................... (22)}$$

The term $\frac{w}{\Delta A}$ represented the contact pressure (p) , and $\frac{dV}{\Delta A}$ represent the increment of wear depth (dh), hence the equation that predicted the wear depth can be concluded.

$$\frac{d\boldsymbol{h}}{dx} = k_D.p \qquad \text{...................................... (23)}$$

where $k_D = \frac{K}{H}$

Hence, Eq.(23) can be rewritten as

$$\boldsymbol{h} = \int k_D.p.\ dx \qquad \text{.................................... (24)}$$

Finite Element Modeling

The finite element analysis code ANSYS was used to solve the non-linear contact problem(ANSYS Manual, 2011). There are several examples of researchers using finite element analysis to simulate wear (Molinari *et al.*, 2001; Ireman *et al.*, 2002; Podra & Anderson, 1999). The equilibrium equation for a nonlinear in a static equilibrium is derived using the principle of virtual work(Mottram & Show, 1996). Thus:

$W_{int.} = W_{ext}$ ....(25)

The virtual internal work is:

$$W_{int.} = \int_V \{\partial\varepsilon\}^T\{\sigma\}.dV \qquad \text{........... (26)}$$

By using the general stress-strain relationship, stresses $\{\sigma\}$, can be determined from the corresponding strains $\{\varepsilon\}$ as:

$\{\sigma\} = [D]\cdot\{\varepsilon\}$ .... (27)

After substituting Eq. (27) into Eq.(26), the virtual internal work can be written as:

$$W_{int.} = \int_V \{\partial\varepsilon\}^T[D]\ \{\varepsilon\}\ dV \qquad \text{............ (28)}$$

The displacements {U} within the element are related by interpolation to nodal displacements {a} by:

$\{U\} = [N]\cdot\{a\}$ .... (29)

By differentiating Eq.(29), the strains for an element can be related to its nodal displacements by:

$$\{\varepsilon\} = [B]\ \{a\} \qquad \text{.......... (30)}$$

where

$[B]$= strain-nodal displacement relation matrix, based on the element shape functions

Assuming that all effects are in the global Cartesian system, and then combining Eq.(30) with Eq.(28) yields:

$$W_{int.} = \{\partial a\}^{T} . \int_{v} [B]^{T} [D]\ [B]\ dV\ .\{a\} \qquad \text{........... (31)}$$

The external work, which is caused by the nodal forces applied to the element, can be accounted for by:

$W_{ext.} = \{a\}^{T}\cdot\{F\}$ .... (32)

Where

{F}= nodal forces applied to the element

Finally, Eqs. (25), (31) and (32) may be combined to give:

$$\{\partial a\}^{T} \int_{v} [B]^{T} [D]\ [B]\ dV\ \{a\} = \{\partial a\}^{T} \{F\} \qquad \text{........... (33)}$$

Noting that $\{\partial a\}^{T}$ vector is a set of arbitrary virtual displacements, the condition required to satisfy Eq.(33) can be reduced to:

$[K^{e}]\cdot\{a\} = \{F\}$ .... (34)

where

$$[K^{e}] = \int_{v} [B]^{T} [D]\ [B]\ dV \qquad \text{........... (35)}$$

$[K^{e}]$ = Element stiffness matrix

$dV = dx\ .\ dy\ .\ dz$

Eq.(34) represents the equilibrium equation on a one-element basis. For all elements, the overall stiffness matrix of the structure $[K]$ is built up by adding the element stiffness matrices (adding one element at a time), after transforming from the local to the (overall) global coordinates, this equation can be written as:

$$[K]\ \{a\} = \{F^{a}\} \qquad \text{......... (36)}$$

where

$[K] = \sum_{n} [K^{e}]$ = overall structural stiffness matrix

$\{F^{a}\} = \{F\}$ = vector of applied loads (total external force vector)

n = total number of elements

Contact Modeling

A three-dimensional nonlinear surface-to-surface "contact-pair" element was used to model the nonlinear behavior of the contact surface between two surfaces at different times. The surface-to-surface element overcomes most of the limitations or restrictions of the other contact elements. The contact-pair consists of the contact between two boundaries, one of the boundaries represents contact, slid and deformable surface taken as contact surface (CONTA-173 in ANSYS) and the other represents rigid surface taken as a target surface (TARGE-170 in ANSYS). The contact element overlays the solid elements and describes the boundary of a deformable body that is potentially in contact with a rigid target surface. Hence, the target is simply a geometric entity in space that senses and responds when the contact element moves into a target segment element. This means that the essential part of the "contact-pair" that represents the contact behavior is a deformable element (i. e., CONTA-173). The target surface is modeled through a set of target segments each having three nodes (triangle segment) and several target segments comprise one target surface, as shown in Fig.(2). The contact element has four corner nodes, and each node has three translation degrees of freedom (u, v and w) in x, y and z directions respectively. This element is located on the surfaces of 3-D solid (such as 8-node brick element) and has the same geometric characteristics as the solid element face with which it is connected as shown in Fig.(2). The contact element is capable of supporting compression in the direction normal to the interface between the two surfaces and Coulomb shear friction in the tangential direction.

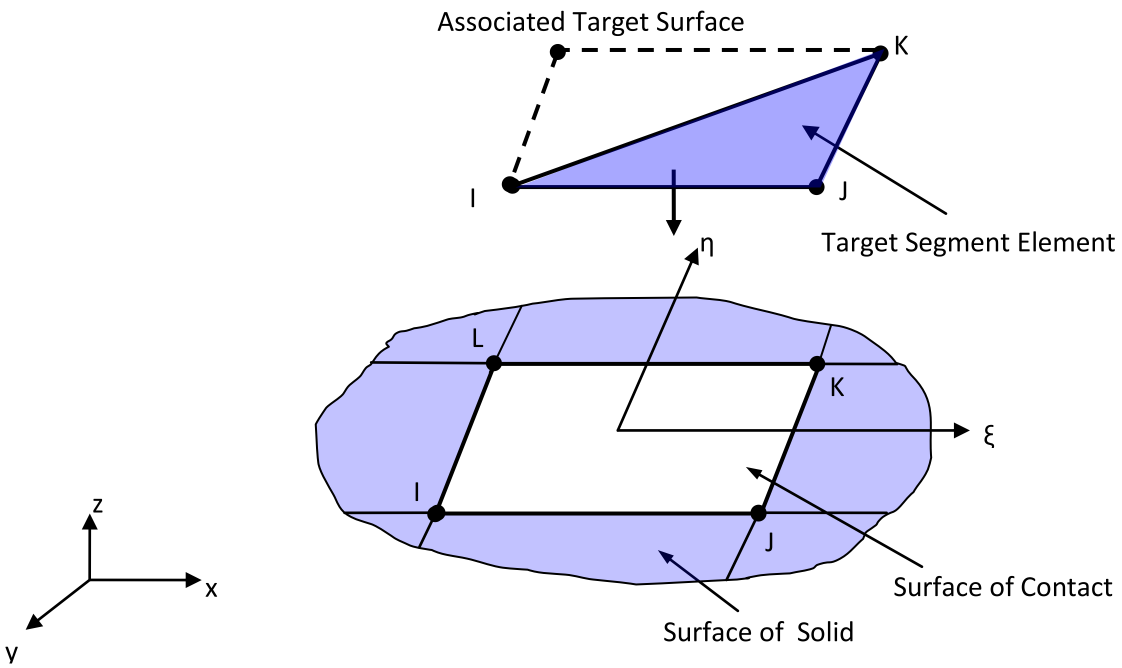

Fig.(2) Surface-to-Surface Contact-Pair Element (ANsys Manual, 2011)

A convergence criterion is required in order to terminate the iterative process required for solving the nonlinear Eq.(36), i.e., a termination criterion for the iterative process should be used to stop the iteration when a sufficient accuracy is achieved or when no further iterations are necessary. Several convergence criteria can be used to control equilibrium; these are the displacement, force and internal energy criteria. Only the force criterion is adopted in the present study. In the force convergence criterion, the norm of the residual forces at end of each iteration is checked against the norm of the current applied forces as: (Johns)

$$\|\{R\}\| = \left(\sum R_i^2\right)^{0.5} \leq T_n\left(\sum {F_i^a}^2\right)^{0.5} \qquad \text{............ (37)}$$

$$\{R\} = \{F^a\} - \{F^{in}\} \qquad \text{...... (38)}$$

where

T_n = tolerance (taken equal to 0.1%)
{R} = residual load vector

The nonlinear finite element analysis used in simulating the response of wear surfaces must include as well a criterion to terminate the analysis when failure of the structure is reached. In a physical test under load control, collapse of a structure takes place when no further loading can be sustained; this is usually indicated in the numerical tests by successively increasing iterative displacements and a continuous growth in the dissipated energy. Hence, the convergence of the iterative process cannot be achieved and therefore it is necessary to specify a suitable criterion to terminate the analysis. In the present study, a maximum number of iterations for each increment of load are specified to stop the nonlinear solution if the convergence tolerance has not been achieved. A maximum number of iterations in the range (25-50) are used, because it is observed and found that this range is generally sufficient to predict the solution's divergence or failure. In the present study, the full Newton-Raphson method was used in analyzing the contact surfaces using finite element method. The movement of the surface was defined using a pilot node; this node was also employed to obtain the applied force during the simulation and material nonlinearity, which results from the nonlinear relationship between stresses and strains.

Cases Studies

Two cases are studied, the first one is for rectangular contact surfaces and the other for circle- rectangle contact surfaces.
Fig.(3) shows the rectangular contact surfaces and circle- rectangle contact surfaces of carbon steel 1020 , where the chemical composition of it shown in Table (1).

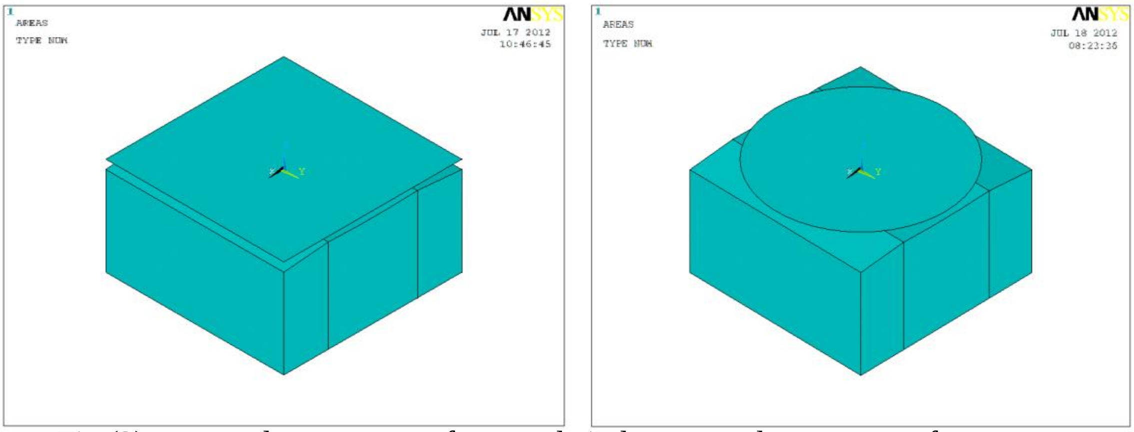

Fig.(3) rectangular contact surfaces and circle- rectangle contact surfaces

Table (1) Chemical composition of carbon steel 1020

element	C%	Mn %	P %	S%	Si%	Ni%	Cr%	Mo %	Cu %	V%
Standard	0.14 - 0.22	0.4 – 0.65	-	-	-	-	0.05	-	-	-
Measured	0.169	0.65	-	0.014	0.019	0.004	0.024	0.054	0.022	0.002

Case – one - Rectangular Contact Surfaces

Two applied load are used (50 kN and 100 kN) for each load , the test is done for four asperities (0.045, 0.055, 0.065,0.07)mm, the results of distribution of contact pressure and wear depth for each time 10, 20, 30, 40, 50, 60, 70, 80 sec are shown in Fig.(4).

A-1 Load 50 kN , Asperity 0.045

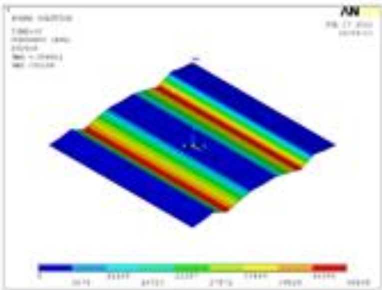

T10.bmp

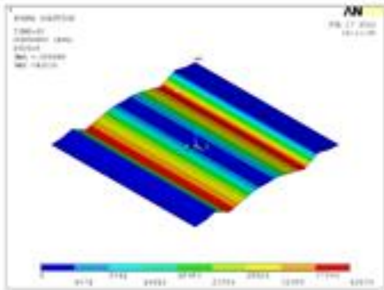

T20.bmp

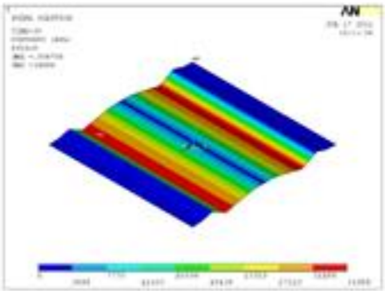

T30.bmp

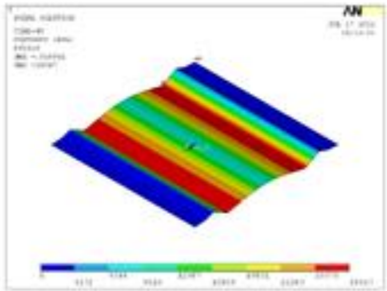

T40.bmp

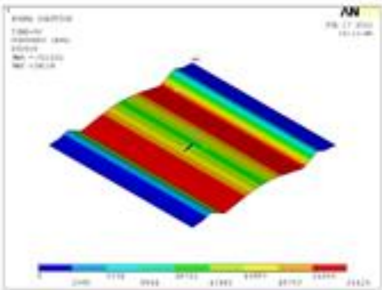

T50.bmp

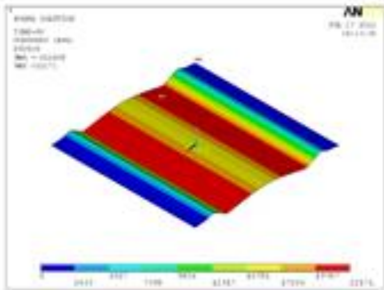

T60.bmp

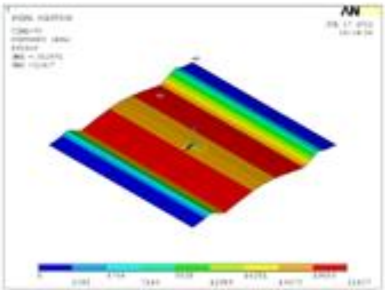

T70.bmp

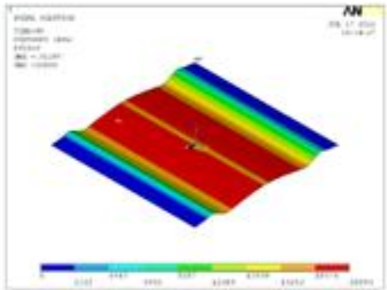

T80.bmp

A-2 Load 50 kN , Asperity 0.055

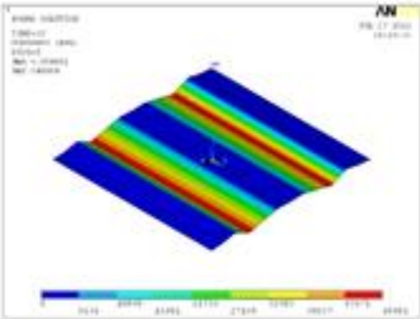

T10.bmp

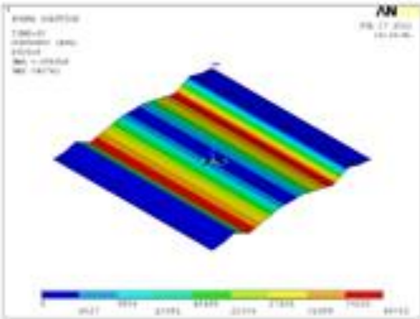

T20.bmp

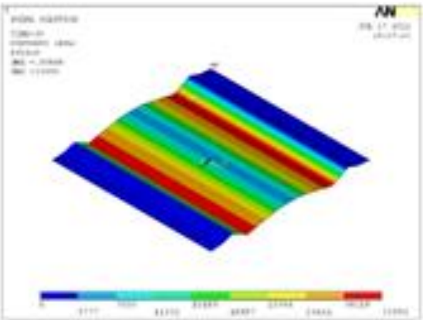

T30.bmp

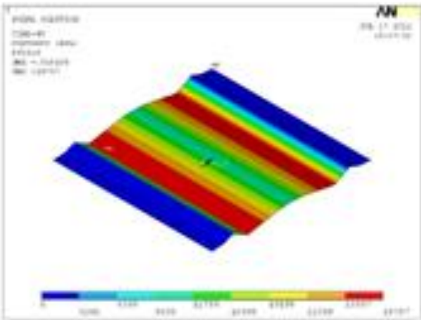

T40.bmp

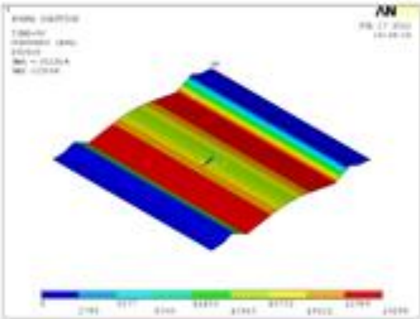

T50.bmp

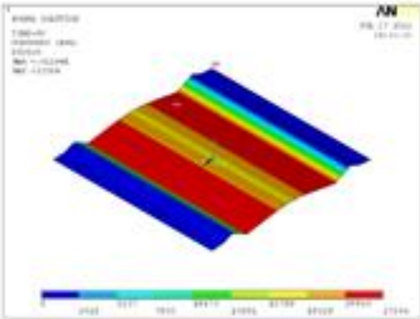

T60.bmp

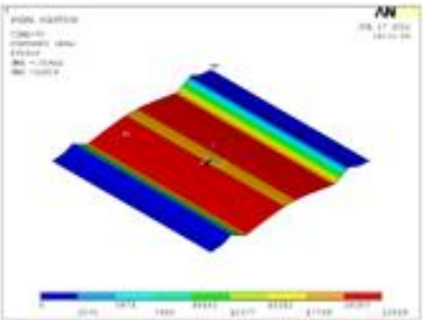

T70.bmp

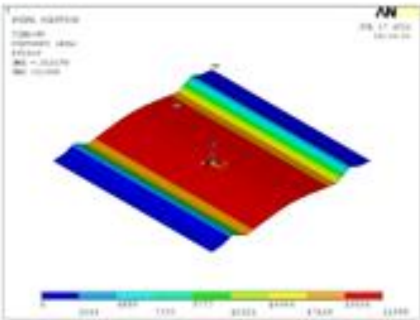

T80.bmp

A-3 Load 50 kN , Asperity 0.065

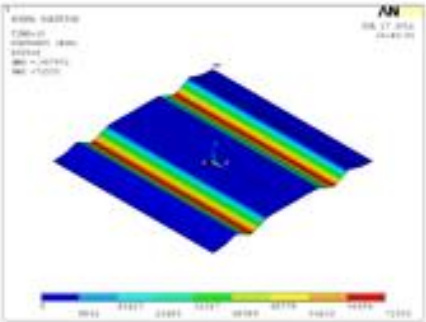

T10.bmp

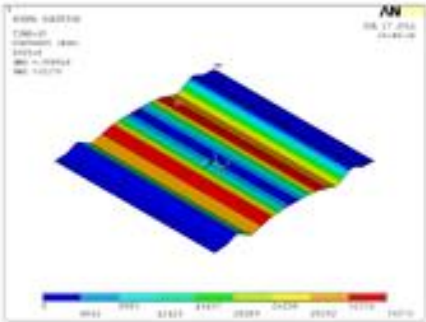

T20.bmp

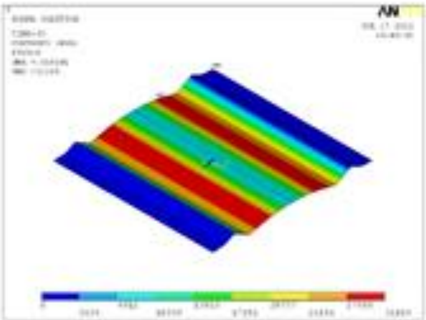

T30.bmp

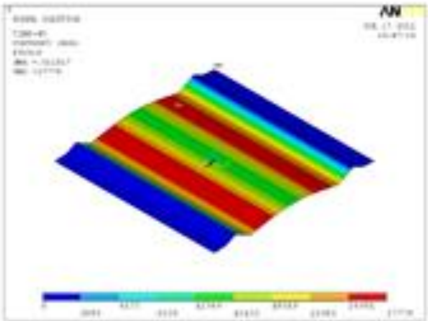

T40.bmp

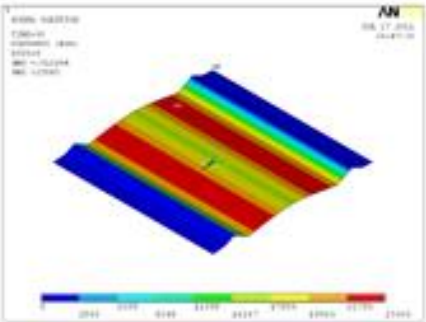

T50.bmp

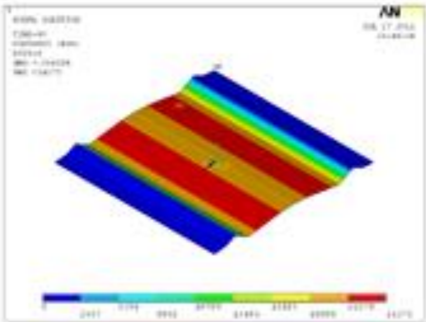

T60.bmp

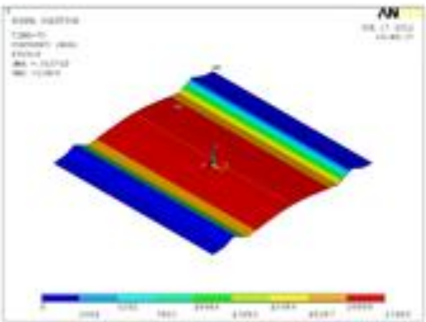

T70.bmp

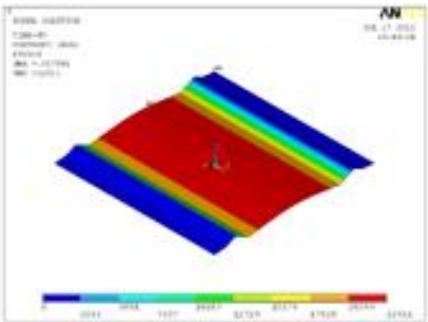

T80.bmp

A-4 Load 50 kN , Asperity 0.07

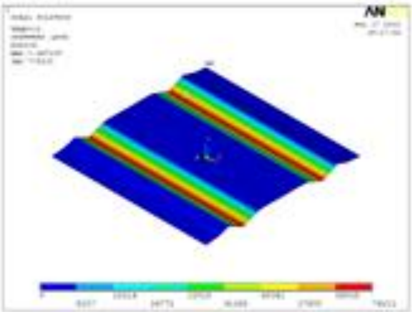

T10.bmp

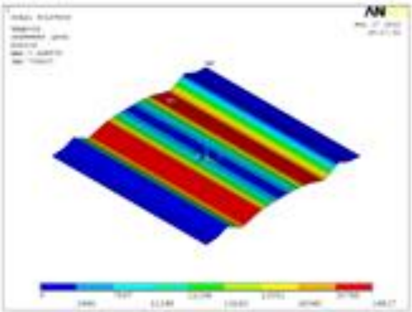

T20.bmp

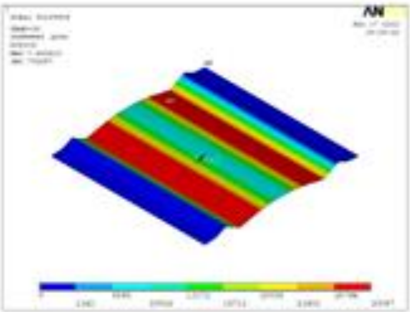

T30.bmp

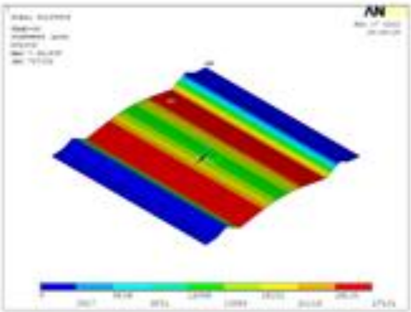

T40.bmp

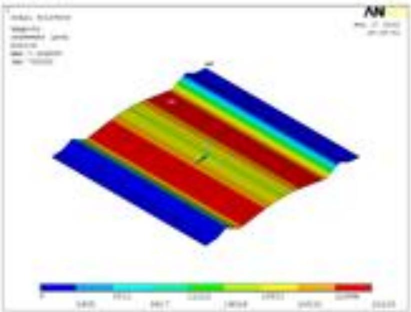

T50.bmp

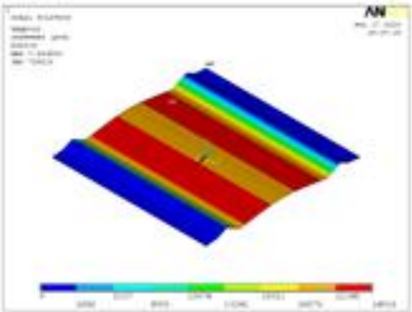

T60.bmp

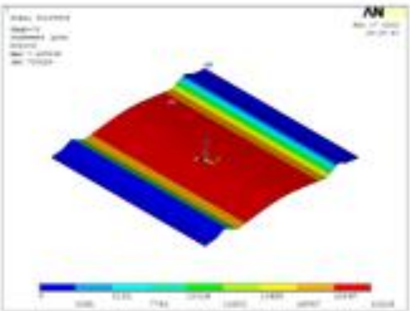

T70.bmp

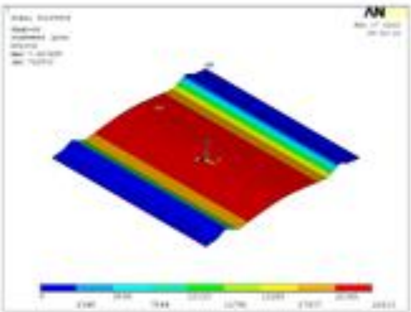

T80.bmp

B-1 Load 100 kN , Asperity 0.045

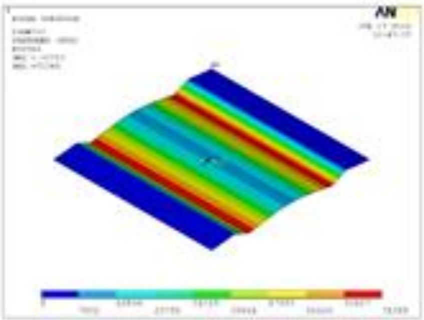

T10.bmp

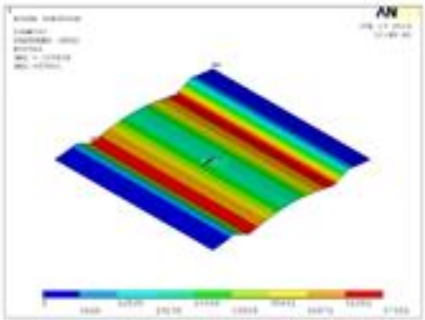

T20.bmp

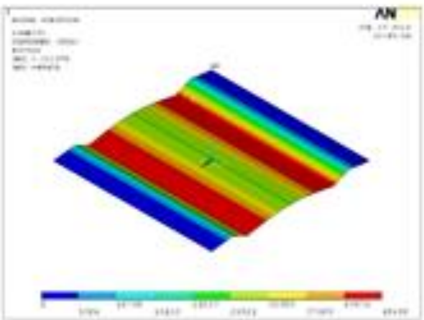

T30.bmp

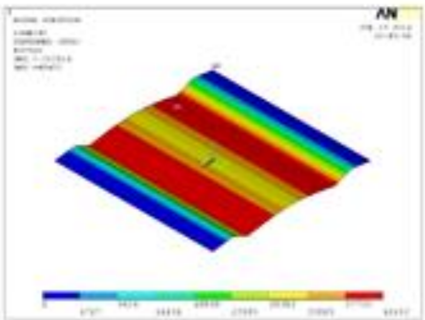

T40.bmp

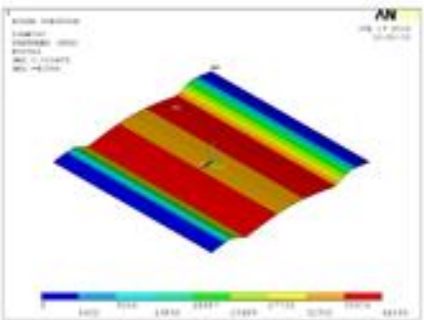

T50.bmp

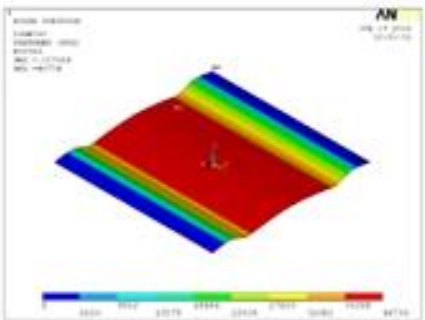

T60.bmp

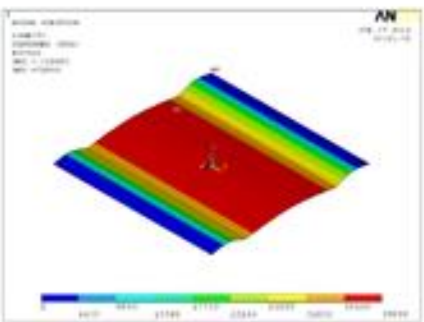

T70.bmp

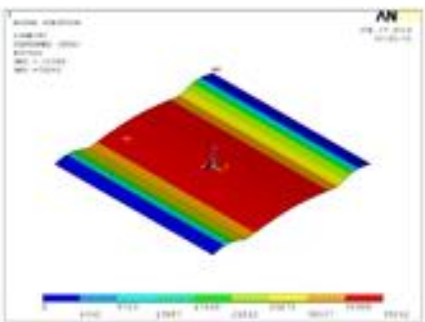

T80.bmp

B-2 Load 100 kN , Asperity 0.055

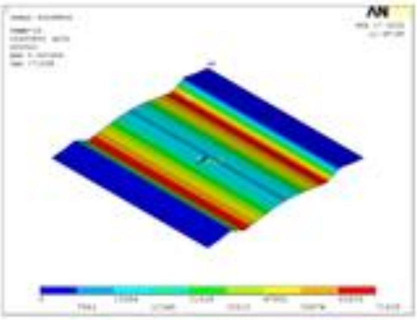

T10.bmp

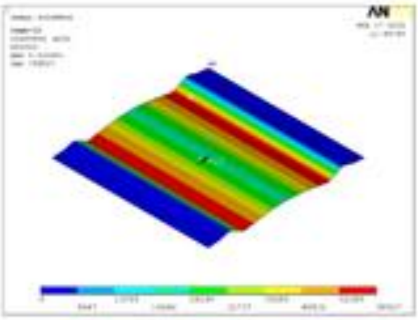

T20.bmp

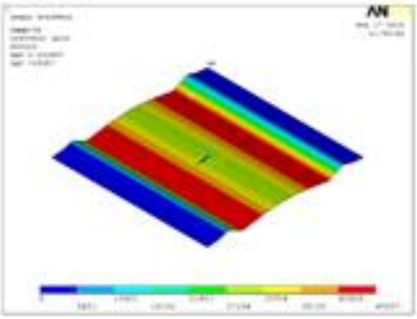

T30.bmp

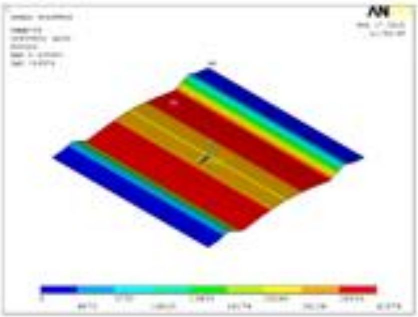

T40.bmp

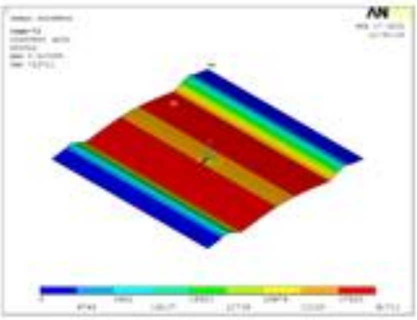

T50.bmp

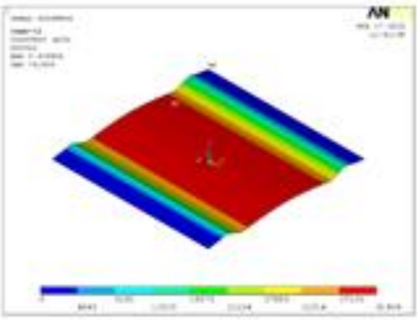

T60.bmp

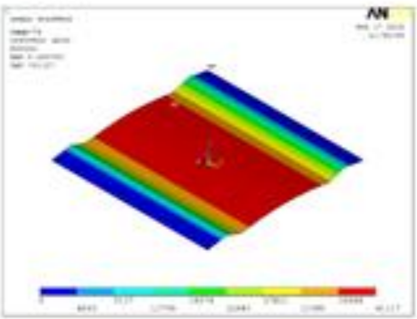

T70.bmp

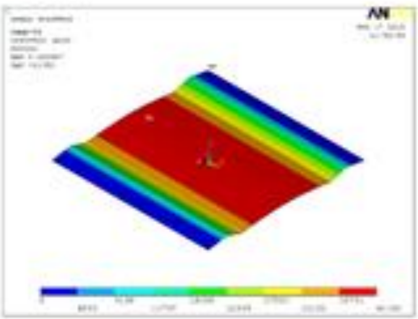

T80.bmp

B-3 Load 100 kN , Asperity 0.065

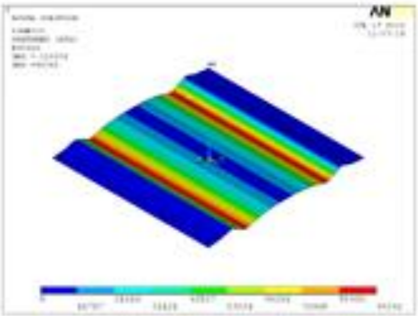

T10.bmp

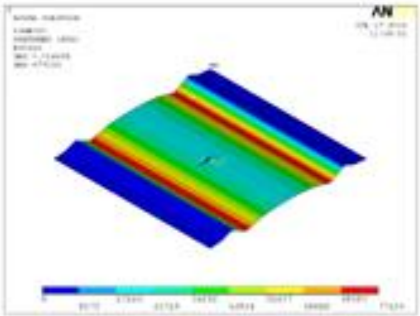

T20.bmp

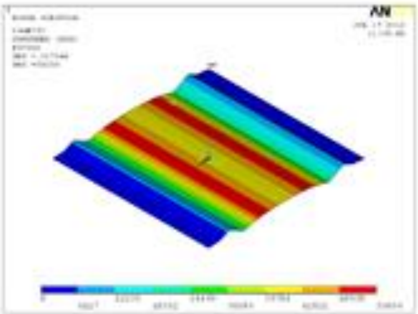

T30.bmp

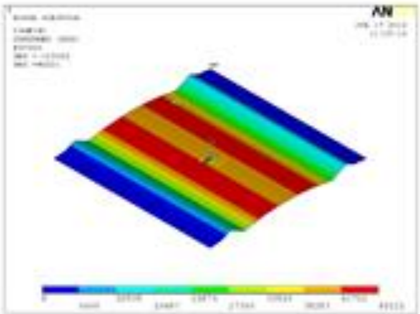

T40.bmp

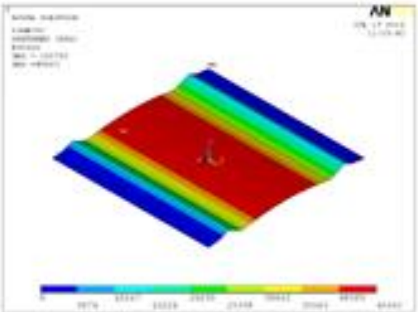

T50.bmp

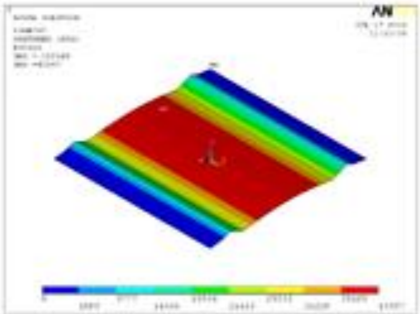

T60.bmp

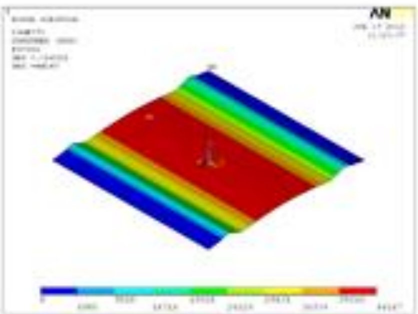

T70.bmp

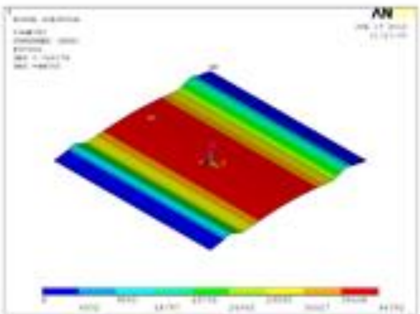

T80.bmp

B-4 Load 100 kN , Asperity 0.07

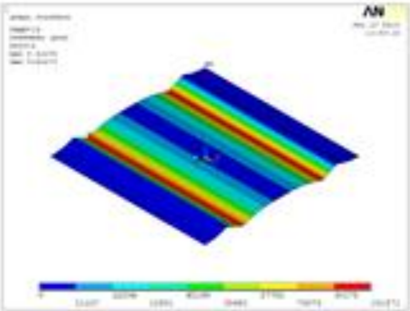

T10.bmp

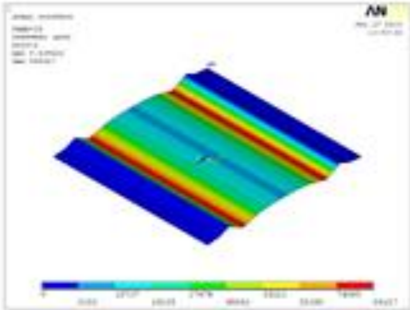

T20.bmp

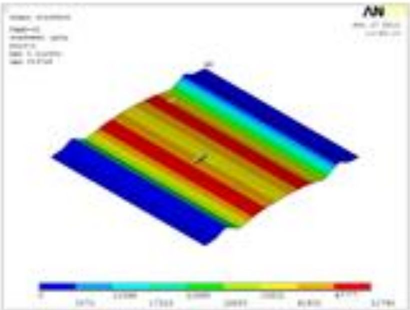

T30.bmp

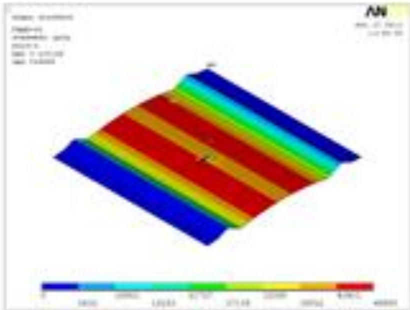

T40.bmp

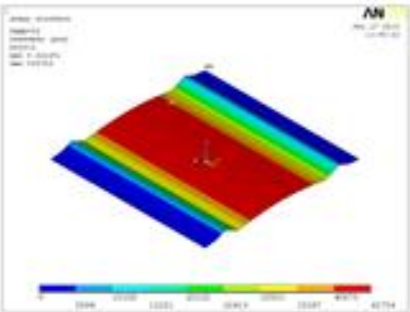

T50.bmp

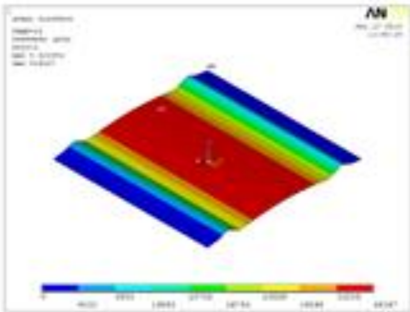

T60.bmp

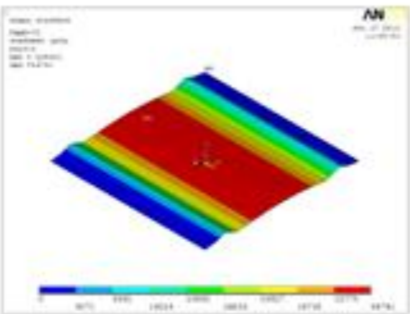

T70.bmp

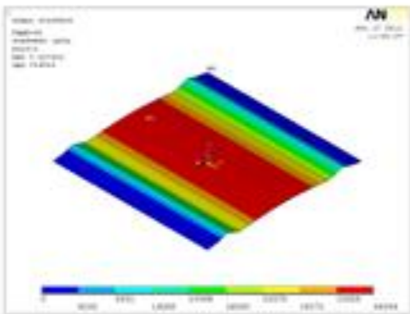

T80.bmp

Case – Two - Circle - Rectangular Contact Surfaces

Two applied load are used (50 kN and 100 kN) for each load , the test is done for four asperities (0.045, 0.055, 0.065,0.07), the results of the distribution of contact pressure and wear depth for each time 10, 20, 30, 40 ,50 ,60 ,70, 80 sec are shown in Fig.(5).

A-1 Load 50 kN , Asperity 0.045

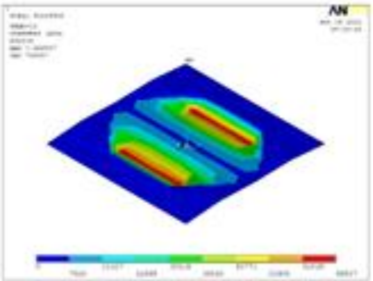

T10.bmp

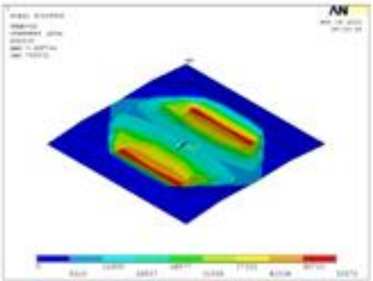

T20.bmp

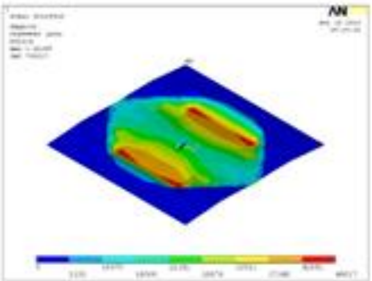

T30.bmp

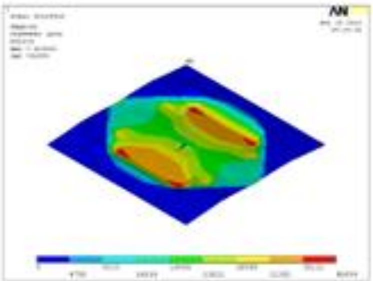

T40.bmp

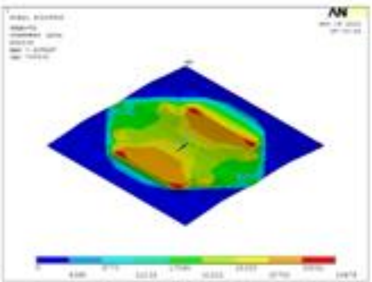

T50.bmp

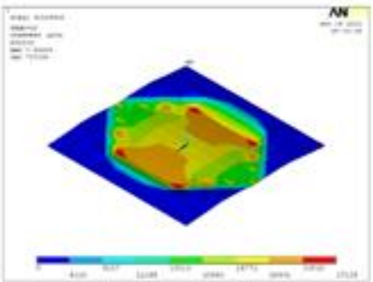

T60.bmp

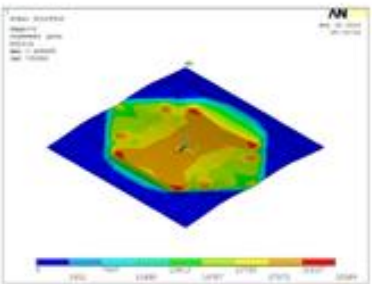

T70.bmp

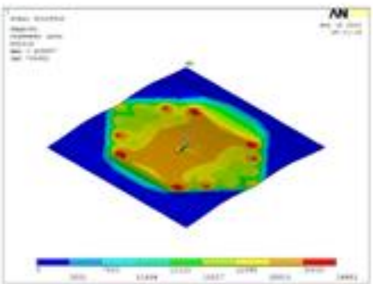

T80.bmp

A-2 Load 50 kN , Asperity 0.055

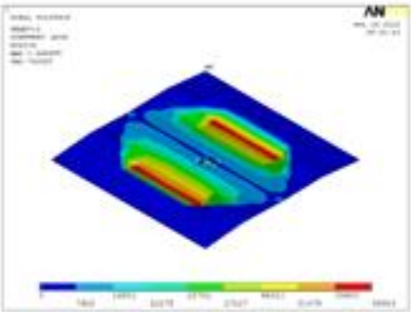

T10.bmp

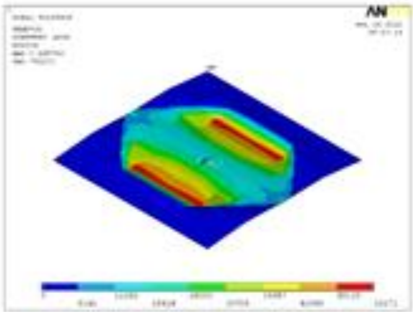

T20.bmp

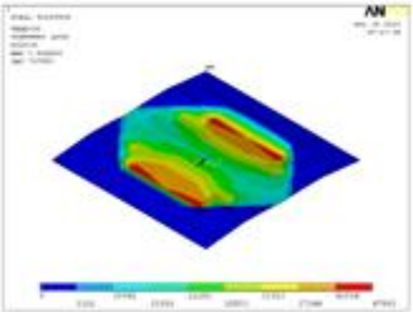

T30.bmp

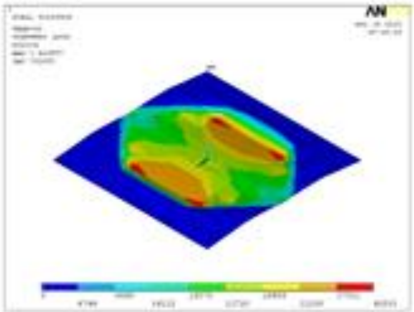

T40.bmp

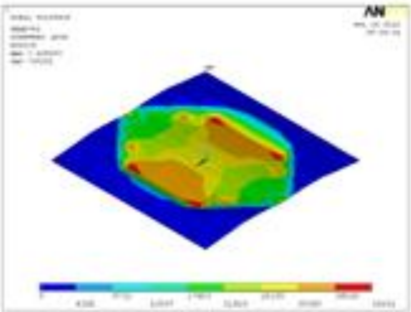

T50.bmp

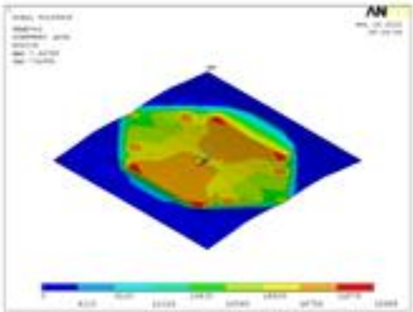

T60.bmp

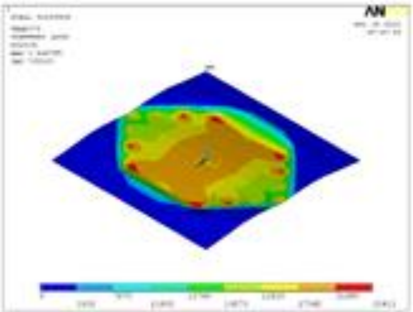

T70.bmp

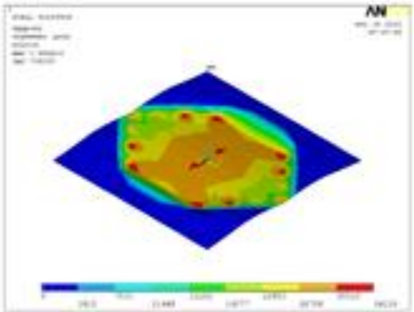

T80.bmp

A-3 Load 50 kN , Asperity 0.065

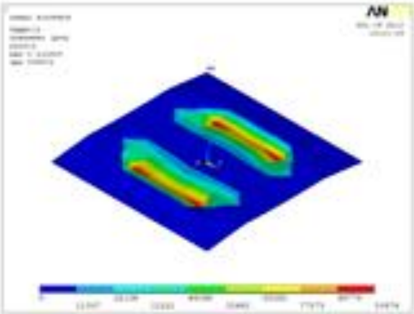

T10.bmp

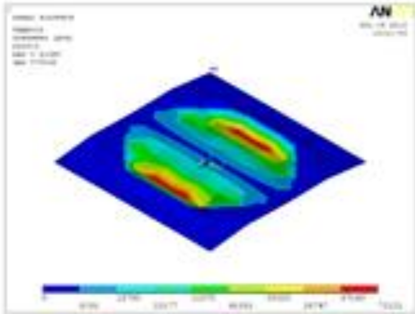

T20.bmp

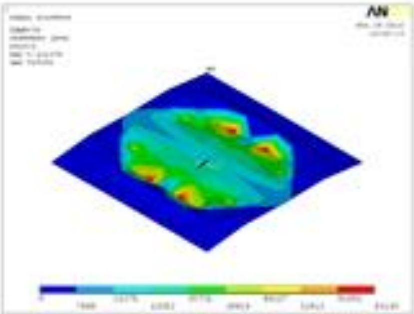

T30.bmp

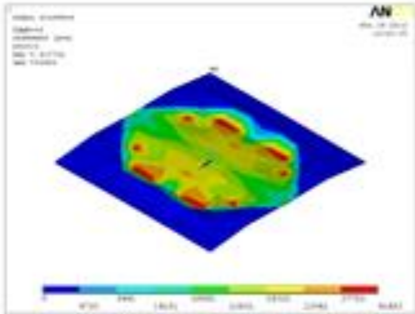

T40.bmp

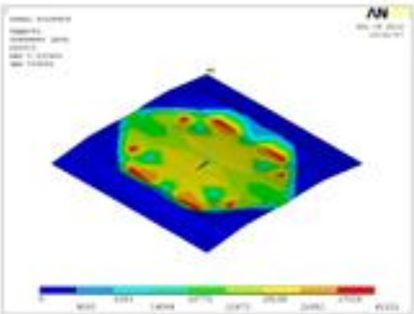

T50.bmp

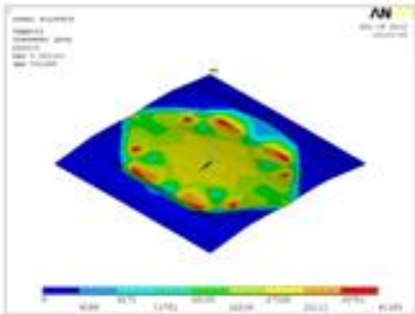

T60.bmp

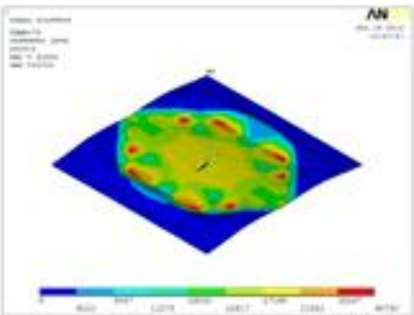

T70.bmp

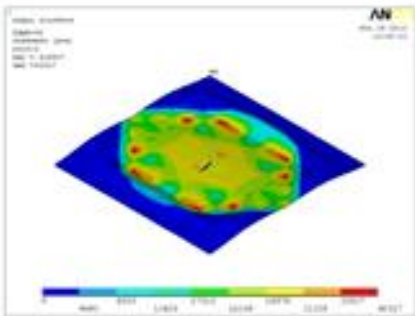

T80.bmp

A-4 Load 50 kN , Asperity 0.07

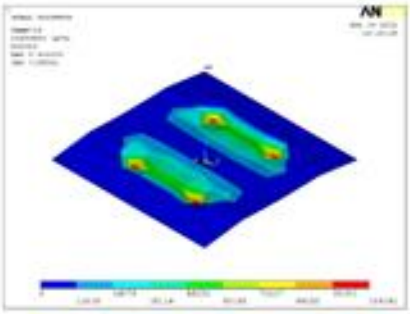

T10.bmp

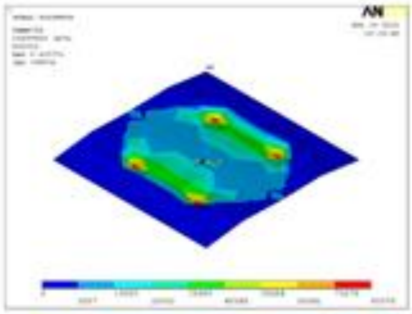

T20.bmp

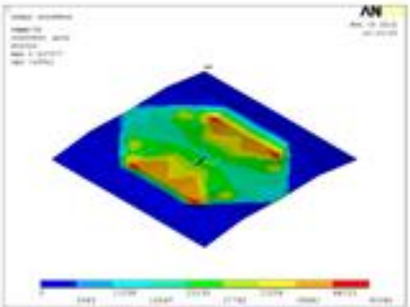

T30.bmp

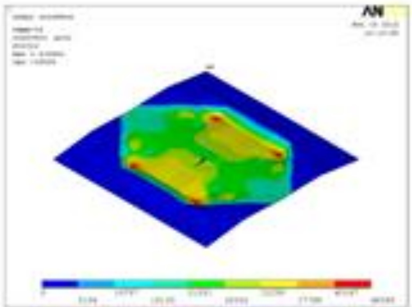

T40.bmp

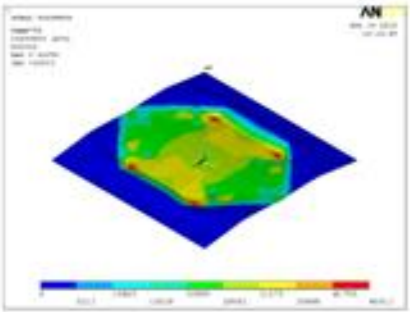

T50.bmp

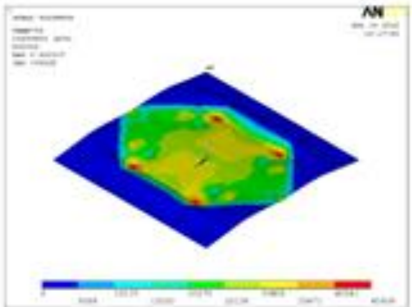

T60.bmp

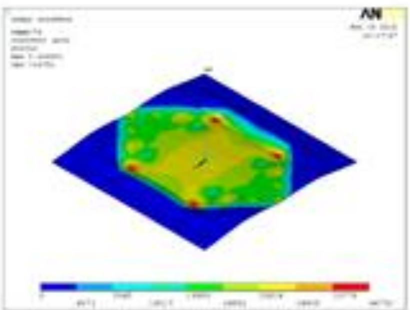

T70.bmp

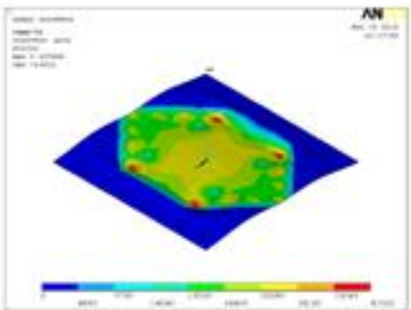

T80.bmp

B-1 Load 100 kN , Asperity 0.045

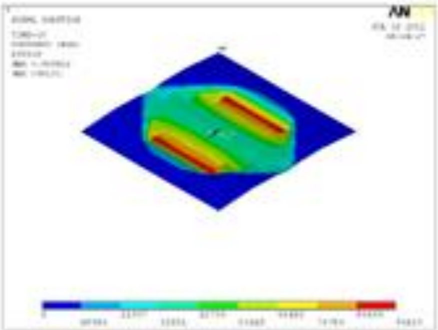

T10.bmp

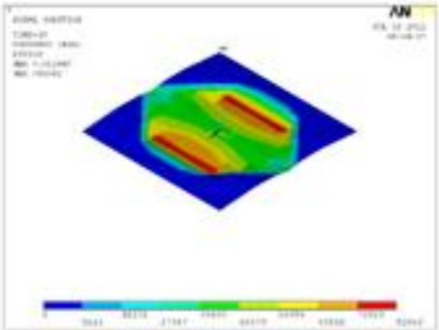

T20.bmp

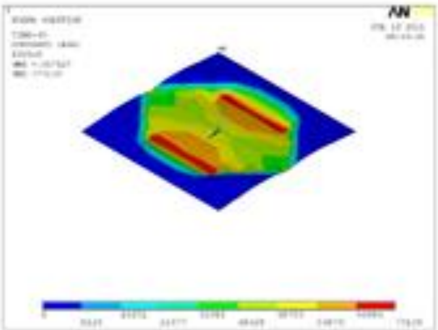

T30.bmp

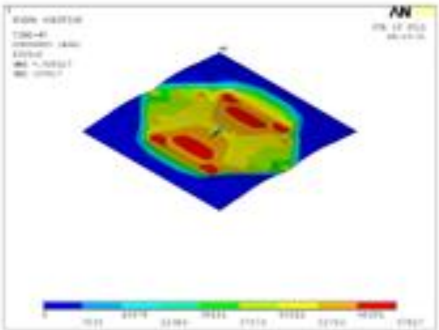

T40.bmp

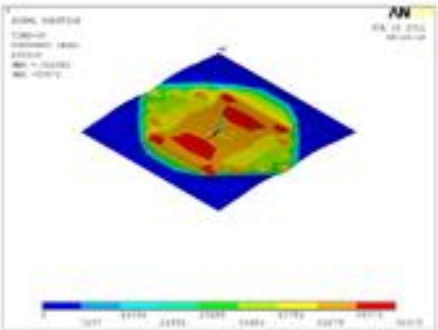

T50.bmp

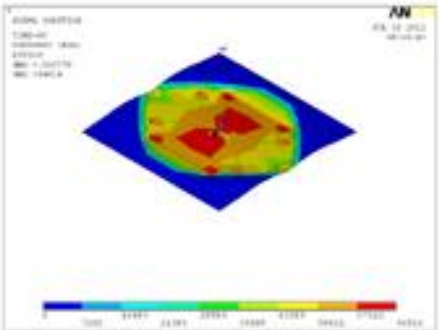

T60.bmp

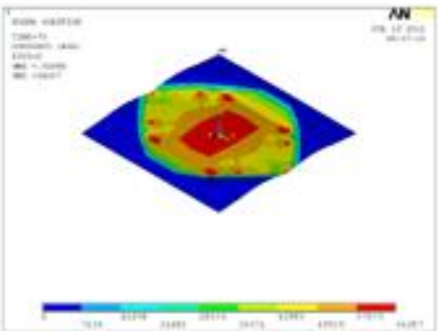

T70.bmp

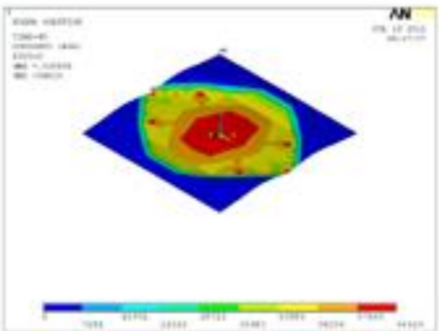

T80.bmp

B-2 Load 100 kN , Asperity 0.055

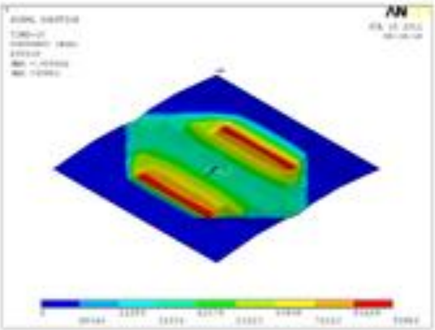

T10.bmp

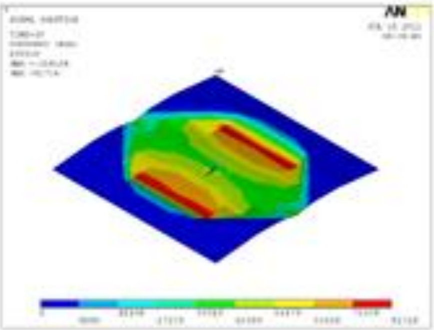

T20.bmp

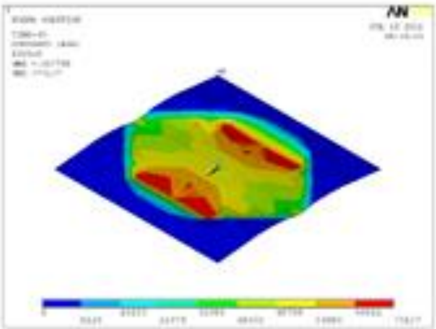

T30.bmp

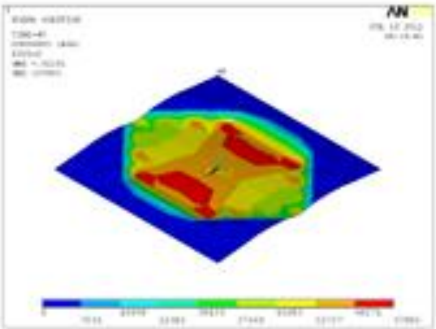

T40.bmp

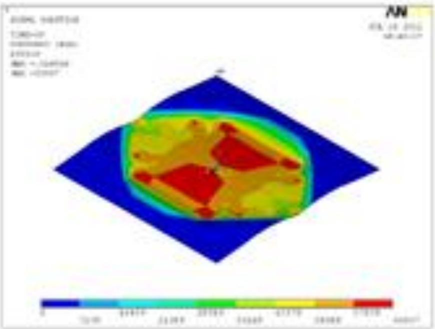

T50.bmp

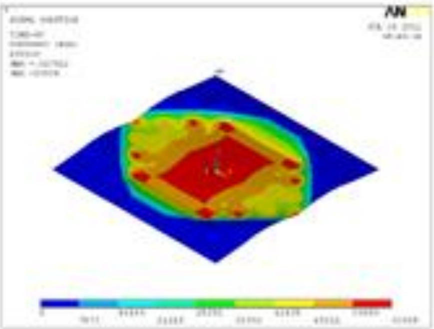

T60.bmp

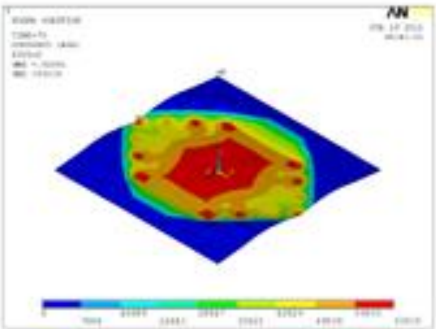

T70.bmp

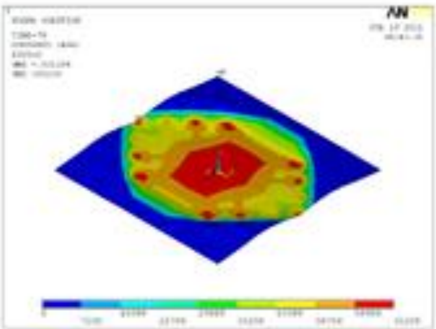

T80.bmp

B-3 Load 100 kN , Asperity 0.065

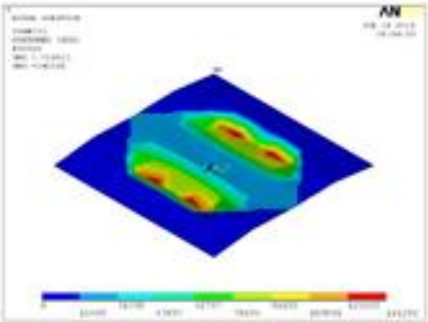

T10.bmp

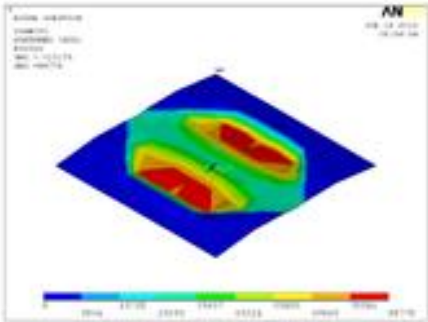

T20.bmp

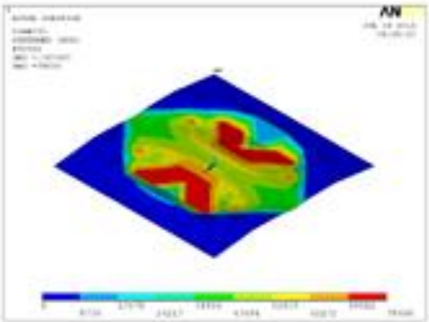

T30.bmp

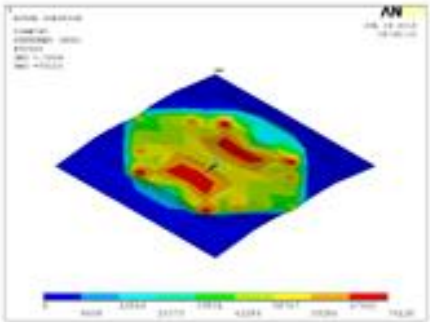

T40.bmp

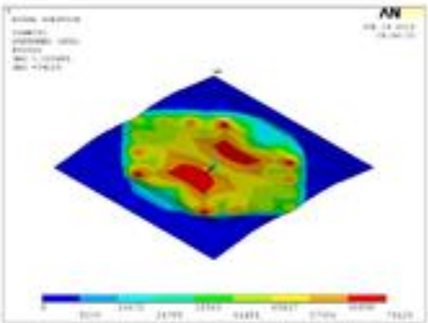

T50.bmp

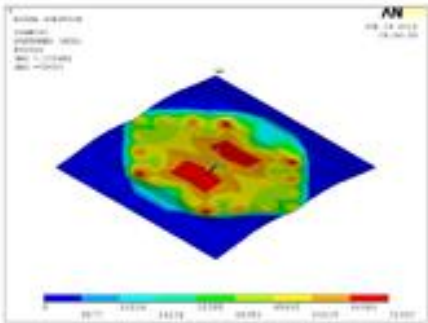

T60.bmp

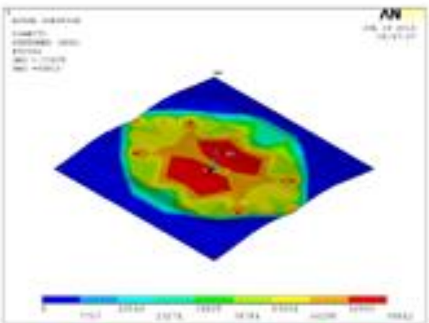

T70.bmp

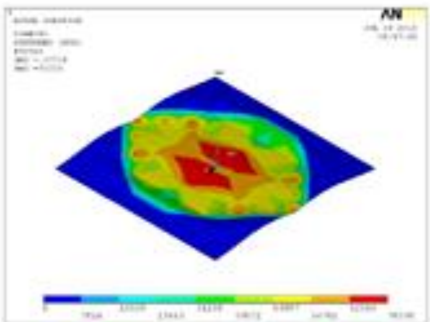

T80.bmp

B-4 Load 100 kN , Asperity 0.07

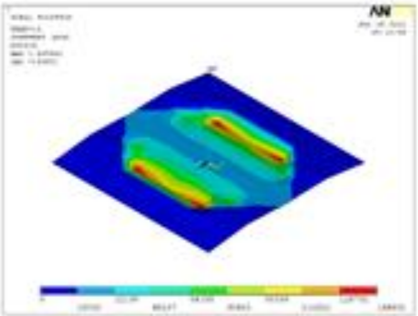

T10.bmp

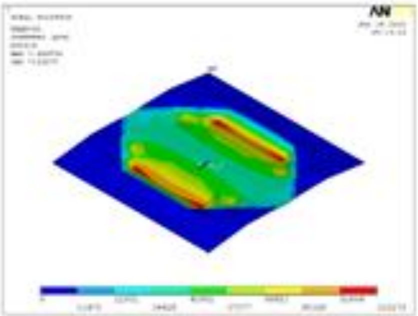

T20.bmp

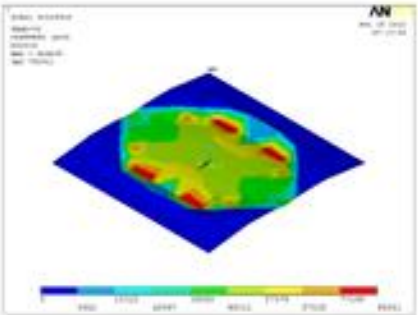

T30.bmp

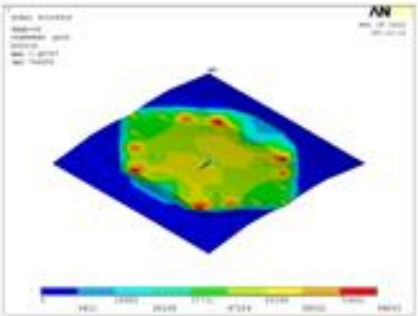

T40.bmp

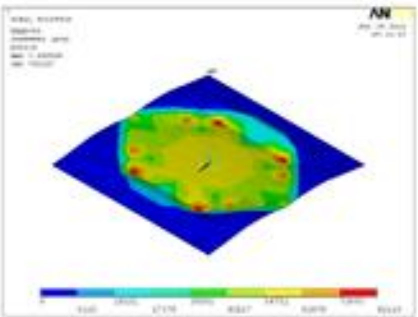

T50.bmp

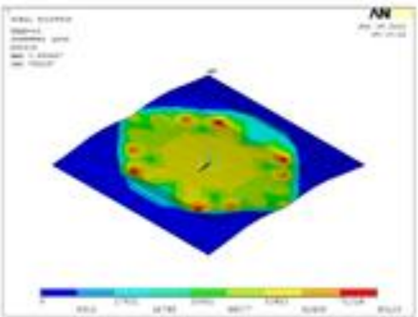

T60.bmp

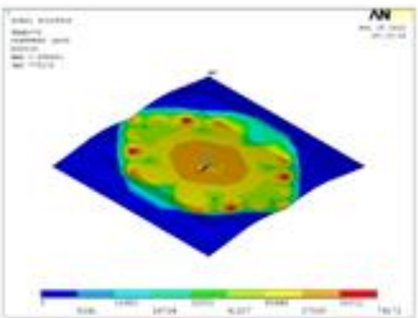

T70.bmp

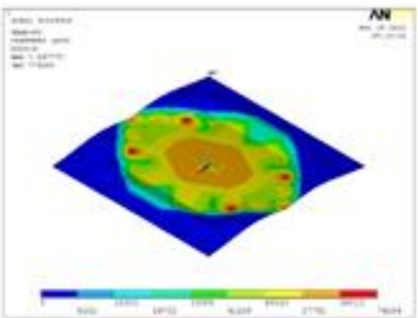

T80.bmp

Discussion

In this paper, an arbitrary lagrangian- eulerian description of contact surfaces has been used to simulate the wear process. The modeling simulates wear as a continuous process, with the contact surfaces updated continuously. The numerical simulation method was proposed to solved wear problems based on Archard model. In order to simulate the evolution of the contact surface profiles with wear cycles for 10, 20, 30, 40, 50, 60, 70, 80 sec, it is necessary to determine the wear depth at each contact node of the finite element model for each time during the wear process, the wear simulation is to discretize a process into several steps. During each step the contact pressure is calculated, then the whole process of wear simulation begins with the calculation of contact pressure between contact surfaces (Eq. 24). Due to the contact problem is a non linear, the finite element code ANSYS 11 is implemented to calculate the contact pressure and (Eq. 24) . Fig.(6) to (9) shows the contact pressure and the wear depth of the two cases with different height of asperities , it can be shown that the wear depth is incresed with the time and the contact pressure is decreased with time for constant applied force, as a general the increased in asperities height caused increasing in wear depth. In the ANSYS simulations, the contact pressure distribution on each element of the two surfaces are obtained as shown in Figs.(4 & 5). It can shown the distribution of contact pressures are different for each time and shape of contact surfaces. Surface–to–surface contact modeling technique that prevents contact elements (CONTA174) and target elements (TARGE170) from penetrating each other is used. In this contact –target strategy the contact pressure is only calculated for nodes on the contact elements. In order to calculated the wear depth on both surfaces. (Figs. 6 to 9).

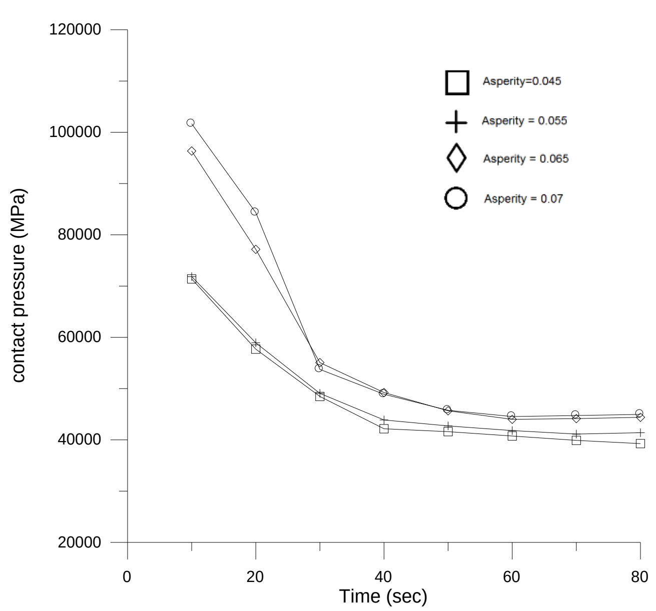

Contact pressure vs time

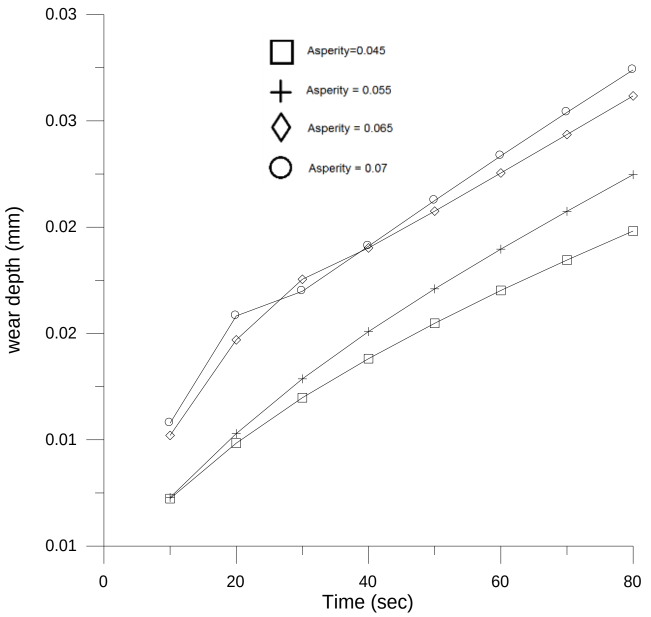

wear depth vs time

Fig-6- Illustrated the Contact pressure and war depth for asperities (0.045, 0.055, 0.065, and 0.07) with applied load 100 kN. (case-1-)

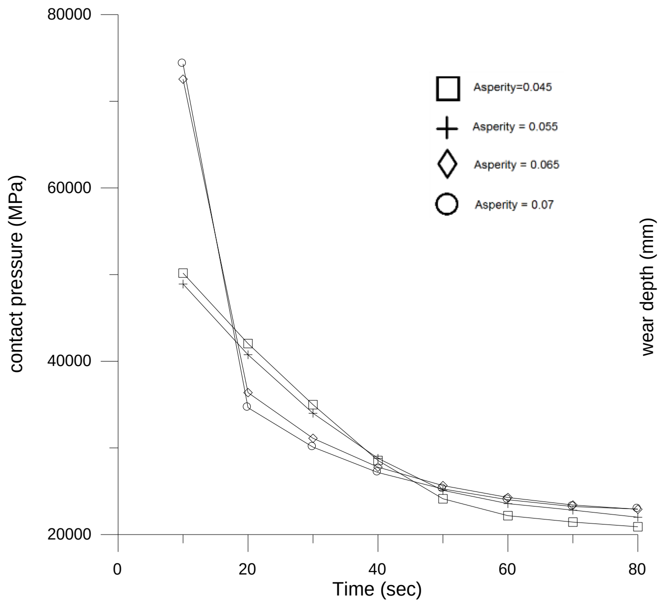

Contact pressure vs time

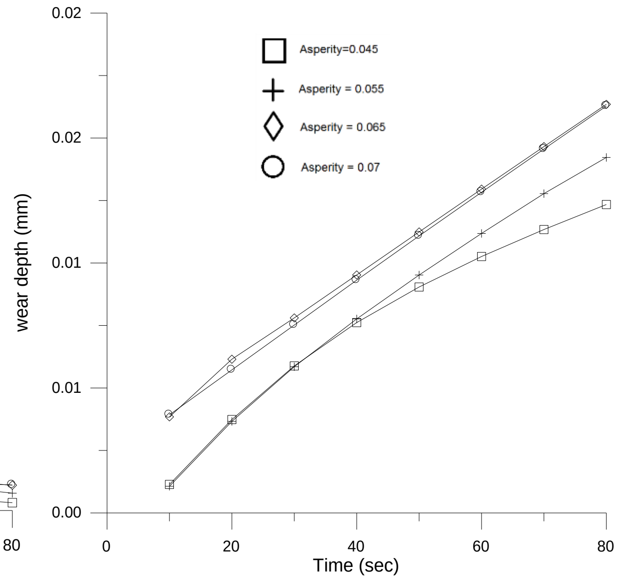

wear depth vs time

Fig-7- Illustrated the Contact pressure and war depth for asperities (0.045, 0.055, 0.065, and 0.07) with applied load 50 kN. (case-1-)

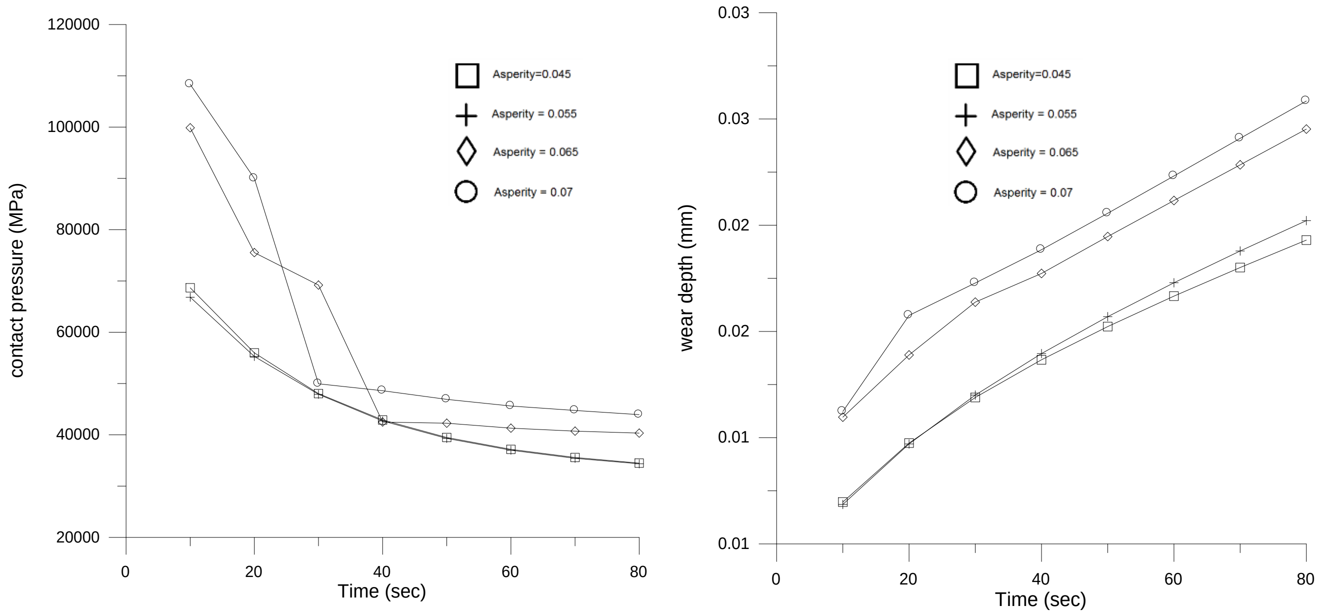

Contact pressure vs time

wear depth vs time

Fig-8- Illustrated the Contact pressure and war depth for asperities (0.045, 0.055, 0.065, and 0.07) with applied load 50 kN. (case-2-)

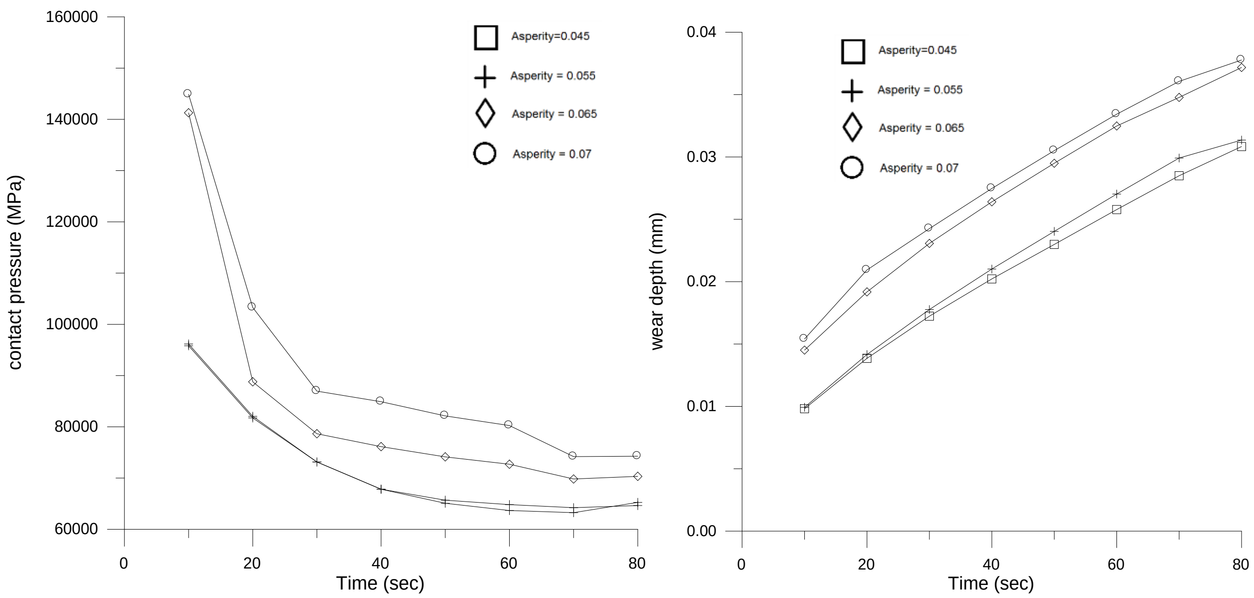

Contact pressure vs time

wear depth vs time

Fig-9- Illustrated the Contact pressure and war depth for asperities (0.045, 0.055, 0.065, and 0.07) with applied load 100 kN. (case-2-)

Conclusions

A finite element analysis model of wear is proposed in this paper. The model is established based on ANSYS software. Archard model is adopted in the wear process which can be analyzed from simulation results of established model. The wear position that would easily occurred can be predicted by the model. Also the wear depth can be predicted for different asperities (0.045, 0.055, 0.065, 0.07)mm. The numerical determination of wear profile was presented in this paper. The influence of the asperities height and the shape of the contact surfaces were studied function of time. It was also concluded that the increased of contact's time caused the wear depth for different asperities increased and vice versa for contact pressure.

References

جون هولنك ، " موفل في عالم الترابيولوجيا" ، ترجمة د. محمد جواد كاظم ، د. مهدي سعيد حيدر ، الجامعة التكنولوجيا ، قسم هندسة الانتاج والمعادن ، 1985، ص (88-104) .

ANSYS Manual, Version (11), USA, 2011.

Archard J.F. " Contact and rubbing of flat surfaces" , J. Appl. Phys., Vol. 24, P. 981-988, 1953.

Biglari F.R. and M. Zamani " Die Wear Profile Investigation in Hot Forging", Proceedings of the World Congress on Engineering , Vol. II , 2008.

Ireman, P. ; Klarbring, A.; Stromberg N. " Finite Element Algorithms for Thermoelastic Wear Problems" Eur. J. Mech. A-Solids, Vol. 21, P.(423-440), 2002.

Johnson, D. H., "Principle of Simulating Contact between Parts using ANSYS", (Web Site).

Kim , D.H.; Lee, H.C.; Kim B.M. and K. H. Kim " Estimation of die service life against plastic deformation and wear during hot forging processes", Journal of Materials Processing Technology, Vol. 166, P. 372-380, 2005.

Molinari, J.F.; Ortiz, M.; Radovitzky, R.A. ; Repetto E. " Finite Element Analysis of Dry Sliding Wear in Metals", Eng. Comput. , Int. J. Comput.-Aided Eng., Vol. 18, P.(592-610), 2001.

Mottram, J. T. and Show, C. T.,"Using Finite Elements in Mechanical Design", 1st Edition, McGraw-Hill Company, UK 1996, P.(276).

Nam Ho Kim, Dongki Won, David Burris, Brian Holtkamp, Gregory R. Gessel, Paul Swanson and W Gregory Sawyer "Finite Element Analysis and Experiments of Metal/ Metal Wear in oscillatory Contacts" Wear , Vol. 258, P. (1787- 1793), 2005.

Podra, P. ; Andersson S. " Simulating sliding Wear with Finite Element Method", Tribol. Int. , Vol.(32), P.(71-81), 1999.

Rabinowicz, E. " Friction and Wear of Materials", John Wiley and Sons, Inc., New York, (1965), p(113-122).

Wang X. Z. and S. H. Masood " Investigation of die radius arc profile on wear behavior in sheet metal processing of advanced high strength steels", Materials and Design, Vol. 32, P. 1118-1128, 2011.

Xuejin SHEN, Lei CAO and Ruyan LI " Numerical Simulation of Sliding Wear Based on Archard Model", IEEE, 2010.